Journal of Renewable and Sustainable Energy

Real-time low-frequency oscillations monitoring

Cite as: J. Renewable Sustainable Energy **13**, 045501 (2021); https://doi.org/10.1063/5.0051338
Submitted: 24 March 2021 . Accepted: 20 June 2021 . Published Online: 20 July 2021

Bin Hu, and Hamid Gharavi

Journal of Renewable and Sustainable Energy | ARTICLE | scitation.org/journal/rse

Real-time low-frequency oscillations monitoring

Cite as: J. Renewable Sustainable Energy **13**, 045501 (2021); doi: 10.1063/5.0051338
Submitted: 24 March 2021 · Accepted: 20 June 2021 ·
Published Online: 20 July 2021

View Online Export Citation CrossMark

Bin Hu[a)] and Hamid Gharavi[b)]

AFFILIATIONS

Advanced Network Technologies, National Institute of Standards and Technology, Gaithersburg, Maryland 20899, USA

[a)]Author to whom correspondence should be addressed: bhu@nist.gov
[b)]Electronic mail: hamid.gharavi@nist.gov

ABSTRACT

A major concern for interconnected power grid systems is low-frequency oscillation, which limits the scalability and transmission capacity of power systems. Undamped or poorly damped oscillations will lead to undesirable conditions or even a catastrophic system blackout. Real-time synchrophasor data can be used to reliably detect and control these low-frequency oscillations in order to mitigate their catastrophic impact. In this paper, two low complexity tracking algorithms are proposed to identify and monitor low-frequency oscillations; namely, a fast subspace tracking algorithm and a gradient descent based fast recursive algorithm. Initially, both methods perform a one-time matrix pencil method on the power spectrum matrix of real-time Phasor Measurement Unit (PMU) data to detect low-frequency oscillations. This is then followed by two different low-complexity algorithms to fast track the low-frequency oscillations. While the first method uses a recursive fast data projection method-based algorithm, the latter runs a gradient-descent based fast recursive algorithm on every PMU to track and monitor low-frequency oscillations. Both methods have been compared to other state-of-the-art techniques, such as matrix pencil method, frequency domain decomposition, and TLS-ESPRIT. We have shown that the proposed approaches are capable of achieving performance with high accuracy, especially in terms of computational complexity for a large system with many PMUs.

Published by AIP Publishing. https://doi.org/10.1063/5.0051338

I. INTRODUCTION

Low-frequency oscillation is becoming a major concern with the interconnection of regional power grid systems and the high penetration of renewable energies. The detection and mitigation of low-frequency oscillation can be best accomplished using real-time, high-precision, time-synchronized measurement data. There are two typical low-frequency oscillations; namely, local modes caused by a single generator or multiple generators within one area, and interarea modes associated with a group of generators among multiple areas.[1,2] Interarea oscillations not only limit transmission capacity on the tie-lines between regional power grids but also endanger the stability of the interconnected power system. Please note that when interarea oscillations occur, the amount of power transferred to tie-lines should be reduced in order to ensure stable and secure system operation.[1] Furthermore, with the increasing deployment of renewable and sustainable energy technologies such as wind power and photovoltaic (PV) power, power systems inertia is affected and their stability can be significantly compromised by the injection of these renewable powers through induction generators and/or electronics converters, resulting in intensified low-frequency oscillations.[1] Therefore, monitoring and mitigating low-frequency oscillations can greatly enhance power systems' reliability, scalability, and transmission capacity, as well as provide better solutions for renewable energies.

Traditional methods, such as Prony analysis, Hilbert–Huang transform (HHT), Kalman filter, and wavelet transform (WT), detect and characterize low-frequency oscillations based on post-disturbance data.[3–7] A Prony analysis method is developed from Fourier analysis method and has a high complexity on the order of $O(N^3)$, where N is the dimension of the data vector. The HHT method is proposed to compute the damping ratios of power system signals in Ref. 8. Its computation complexity is on the order of $O(N\log N)$, which slows down its performance. A Kalman filtering-based technique is used to detect oscillations in large-scale power systems in Ref. 7. It estimates frequency and damping from the on-line measurement signals of PMUs, but at the expense of higher computational complexity, i.e., $O(N^3)$. The WT method with a low complexity of $O(N)$ was used to analyze the dynamic behavior of the power system in Ref. 9. These traditional methods, however, can only detect system disturbance under the system fault occurrence and are not good at detecting disturbance-independent low-frequency oscillations.[1] In order to detect system oscillations without causing big disturbance to power system, some system-identification type methods used probing signals to provide eigenvalue estimation in Ref. 10.

With the implementation of wide area measurement system (WAMS), it is now possible to monitor the oscillations in real time[11–13] by acquiring ambient data using synchronized PMU measurements throughout the power system in a nonintrusive manner. Recently, linear system models, such as autoregressive (AR),[14] autoregressive moving average (ARMA) with the complexity of $O(N\log N)$,[6] together with stochastic state space[15] are used to process ambient PMU measurements under normal operating condition. However, those methods do not perform well in the presence of noise.

Recursive methods, such as least-mean-square (LMS) adaptive filtering with complexity of $O(N)$,[16] robust-recursive-least-square (RRLS) and regularized RRLS (R3LS) with complexity of $O(N^2)$[17,18] update coefficients for each new sample of data and process data in the time domain. In contrast, frequency-domain decomposition (FDD)[19–22] carries out singular value decomposition (SVD), or eigenvalue decomposition (EVD) to the ambient PMU measurements in the frequency domain. Moreover, unlike the previously mentioned time-domain methods, which have to handle data from each PMU separately, the FDD approach can easily detect interarea oscillations by performing SVDs on the power spectral density (PSD) matrix of the entire power system. Another frequency domain method is the Yule–Walker spectrum (YWS) method,[4] which was proposed to calculate autocorrelations from power PSD and is compared with the subspace state-space system identification (N4SID) method.[4] However, those methods are not suitable for adaptive tracking of nonstationary low-frequency oscillations. This is because the required repetitive computation of the subspace or the eigenvectors is at least $O(N^3)$. This complexity is too excessive to practically run in recursive mode. The ESPRIT-based method, with similar complexity to Prony analysis,[23,24] uses least-square or total least squares (TLS) variation to estimate the modes. Its main problem is separating dominant modes from the trivial modes.[25]

The matrix pencil method (MPM) proposed in Ref. 26 is one of the Prony-like methods. It uses SVD on the Hankel matrix to estimate the oscillation components and achieves a better noise performance than the Prony method.[11] However, the SVD approach has a high complexity of $O(N^3)$, which makes MPM very time-consuming, hence is not feasible to track oscillation components in real time. In order to reduce the complexity, subspace tracking algorithms[27–30] are proposed to recursively update the subspace in a sample-by-sample fashion. Their main objective is to directly track components of the eigenvalue decomposition, rather than carrying out eigenvalue decomposition for each block (window) of the power signal samples. Because of their low complexity, subspace tracking algorithms have been widely used in signal processing fields, such as spectrum analysis, direction-of-arrival (DOA) estimation, interference mitigation, radar, and sonar.

In this paper, we present a fast subspace tracking algorithm to identify and monitor low-frequency oscillations. For instance, to detect low-frequency oscillations, an MPM is first performed on the power spectrum matrix from real-time PMU measurements. This is then followed by a low-complexity fast subspace tracking algorithm [on the order of $O((L+1)K)$] to monitor the low-frequency oscillations in real time, where L and K are the pencil parameter and the model order. Moreover, a gradient descent based fast recursive algorithm is proposed to further reduce the computation complexity, where the MPM on the power spectrum matrix of PMU measurements is used to estimate the initial value of oscillation frequencies and damping factors. This is then followed by a low complexity tracking algorithm on the order of $O(K)$. The computational complexity and the convergence speed in which low-frequency oscillations are detected play a crucial role in real-time monitoring of the grid system. Indeed, under these conditions, the control system would be able to respond quickly in order to prevent possible cascading failures or blackouts.

Our major contributions are listed as follows:

(1) Our paper is the first of its kind to use the fast data projection method (FDPM) algorithm27 for low-frequency oscillation monitoring.
(2) In order to detect inter-area oscillations, the proposed FDPM is also expanded to track the subspace of the entire power grid system.
(3) By using the MPM on the spectrum of the whole system in the initial stage, the gradient descent based tracking algorithm can easily identify and track the inter-area oscillations.
(4) The gradient descent based tracking algorithm includes the estimation and tracking of the damping factor, which is a very important parameter used to assess low-frequency oscillations.
(5) We have shown that the proposed tracking algorithms are capable of quickly detecting low-frequency oscillations, hence preventing possible cascading failures in a timely manner. In addition, since highly scalable, they can be used in large power grid systems.

The paper is organized as follows: In Sec. II, a background of the matrix pencil method (MPM) is provided. We then present our fast subspace tracking algorithm in Sec. III, followed by a low complexity gradient descent based tracking algorithm in Sec. IV. Section V provides the simulation results of the proposed tracking algorithms and then the conclusion is presented in Sec. VI.

II. MATRIX PENCIL METHOD FOR SPECTRUM ESTIMATION

The matrix pencil method has been widely used mainly in the field of spectrum analysis and signal parameter estimation. In Fig. 1, an example of spectrum estimation for low-frequency oscillations is

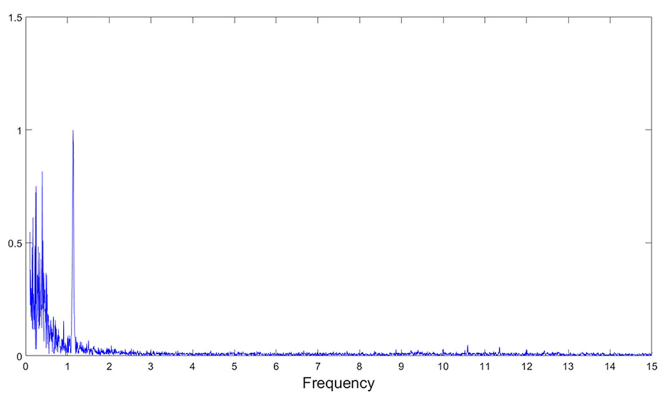

FIG. 1. An example of spectrum estimation for low-frequency oscillations.

displayed.[1] A general model of low-frequency oscillations can be expressed as[2]

$$y(t) = Ae^{(\alpha + j2\pi f)t}, \tag{1}$$

where A denotes the amplitude of the oscillation, α is the damping factor, and f is the oscillation frequency. The low-frequency oscillations typically vary in the range of 0.1–2.0 Hz.[2] Based on damping factor and oscillation frequency, we can derive damping ratio ζ as follows:

$$\zeta = \frac{-\alpha}{\sqrt{\alpha^2 + (2\pi f)^2}}, \tag{2}$$

which is a practical parameter used to assess low-frequency oscillations. Power systems with damping ratio ζ less than 5% are unstable,[31] leading to a high risk of system blackout. When sampled at a constant period T_s, the n th element of the output $\boldsymbol{y}$ can be expressed in the following discrete form:

$$y(n) = \sum_{i=1}^{K} A_i e^{(\alpha_i + j2\pi f_i)nT_s} + n(nT_s), \tag{3}$$

where K is the model order, A_i, α_i, and f_i are the amplitude, damping factor, and frequency of the ith oscillation, respectively. $n(t)$ is the additive Gaussian white noise (AWGN). Figure 2 displays an example of an output vector $\boldsymbol{y}$ constructed from ambient PMU measurements.

If the signal is noise free, output $\boldsymbol{y}$ can be expressed as

$$\boldsymbol{y} = \begin{bmatrix} y(0) \\ y(1) \\ \cdots \\ y(N-1) \end{bmatrix} = \begin{bmatrix} 1 & 1 & \cdots & 1 \\ z_1 & z_2 & \cdots & z_K \\ \vdots & \vdots & \ddots & \vdots \\ z_1^{N-1} & z_2^{N-1} & \cdots & z_K^{N-1} \end{bmatrix} \begin{bmatrix} A_1 \\ A_2 \\ \cdots \\ A_K \end{bmatrix}, \tag{4}$$

where $z_k = e^{(\alpha_k + j2\pi f_k)T_s}$. In the matrix pencil method, an output matrix $\boldsymbol{Y}$ is defined as

$$\boldsymbol{Y} = \begin{bmatrix} y(0) & y(1) & \cdots & y(L) \\ y(1) & y(2) & \cdots & y(L+1) \\ \vdots & \vdots & \ddots & \vdots \\ y(N-L-1) & y(N-L) & \cdots & y(N-1) \end{bmatrix}, \tag{5}$$

where $K \le L \le N-K$ is the pencil parameter. According to Ref. 26, a correctly selected pencil parameter can significantly reduce noise

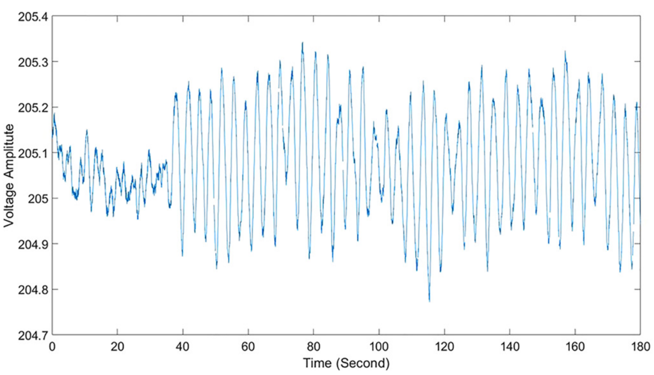

FIG. 2. An example of an output vector $\boldsymbol{y}$ from ambient PMU measurements.

sensitivity. We use $\frac{N}{3}$ for L to ensure the robustness to noise. The singular value decomposition (SVD) of $\boldsymbol{Y}$ can be expressed as

$$\boldsymbol{Y} = \boldsymbol{U\Lambda V}^H, \tag{6}$$

where $\boldsymbol{U}$ and $\boldsymbol{V}$ are orthonormal matrices consisting of eigenvectors of $\boldsymbol{YY}^H$ and $\boldsymbol{Y}^H\boldsymbol{Y}$. $\boldsymbol{\Lambda}$ is a diagonal matrix containing K nonzero singular values of $\boldsymbol{Y}$ in descending order. The superscript H denotes conjugate transpose. In the presence of noise, the zero singular values in $\boldsymbol{S}$ become nonzero but are very close to zero. The model order K can be estimated by finding all singular values which are greater than a threshold, such as $\frac{\sigma_{\max}}{10^r}$, where $\sigma_{\max}$ is the largest singular value and r is the number of significant decimal digits. Singular values below this threshold are set to zero to eliminate the interference from noise.

After discarding the singular values and vectors corresponding to the noise, we can rewrite $\boldsymbol{Y}$ as

$$\boldsymbol{Y}_T = \boldsymbol{U}_S\boldsymbol{\Lambda}_S\boldsymbol{V}_S^H, \tag{7}$$

where $\boldsymbol{U}_S = [\boldsymbol{u}_1, \boldsymbol{u}_2, \ldots, \boldsymbol{u}_K]$ contains column vectors of $\boldsymbol{U}$ corresponding to the K dominant singulars. Signal subspace $\boldsymbol{V}_S = [\boldsymbol{v}_1, \boldsymbol{v}_2, \ldots, \boldsymbol{v}_K]$ contains column vectors of $\boldsymbol{V}$ corresponding to the K dominant singulars and $\boldsymbol{\Lambda}_S$ is a $K \times K$ diagonal matrix containing K nonzero singular values of $\boldsymbol{Y}$. By deleting the last column or the first column of $\boldsymbol{Y}_T$, respectively, we can construct a pair of matrices of $\boldsymbol{Y}_1$ and $\boldsymbol{Y}_2$ as follows:

$$\boldsymbol{Y}_1 = \boldsymbol{U}_S\boldsymbol{\Lambda}_S\boldsymbol{V}_{S,1}^H, \tag{8}$$

$$\boldsymbol{Y}_2 = \boldsymbol{U}_S\boldsymbol{\Lambda}_S\boldsymbol{V}_{S,2}^H, \tag{9}$$

where $\boldsymbol{V}_{S,1}$ **and** $\boldsymbol{V}_{S,2}$ are obtained by deleting the last row and the first row of $\boldsymbol{V}_S$, respectively. It is shown in Ref. 11 that $z_k = e^{(\alpha_i + j2\pi f_i)T_s}$ can be estimated by calculating the eigenvalues of the $K \times K$ matrix $\boldsymbol{V}_{S,2}^H\left[\boldsymbol{V}_{S,1}^H\right]^\dagger$, where $\dagger$ denotes pseudoinverse. After deriving z_k, we can calculate the amplitude A_i by solving Eq. (4).

In order to analyze the spectrum of the entire power grid system, multiple $(N-L) \times (L+1)$ the output matrix can be shown as

$$\boldsymbol{Y}_p = \begin{bmatrix} y_p(0) & y_p(1) & \cdots & y_p(L) \\ y_p(1) & y_p(2) & \cdots & y_p(L+1) \\ \vdots & \vdots & \ddots & \vdots \\ y_p(N-L-1) & y_p(N-L) & \cdots & y_p(N-1) \end{bmatrix}, \tag{10}$$

where, $p = 1, 2, \ldots, P$. These are collected from P PMUs distributed over the grid system, which are used to construct an aggregated $P(N-L) \times (L+1)$ output matrix: $\boldsymbol{B} = [\boldsymbol{Y}_0^H\ \boldsymbol{Y}_1^H \ldots \boldsymbol{Y}_P^H]^H$. The singular value decomposition (SVD) of $\boldsymbol{B}$ can be expressed as

$$\boldsymbol{B} = \boldsymbol{\Gamma\Sigma\Pi}^H, \tag{11}$$

where $\boldsymbol{\Gamma}$ and $\boldsymbol{\Pi}$ are orthonormal matrices consisting of eigenvectors of $\boldsymbol{BB}^H$ and $\boldsymbol{B}^H\boldsymbol{B}$. Similarly, after discarding the singular vectors corresponding to the noise in $\boldsymbol{\Pi}$, we can obtain the signal subspace $\boldsymbol{\Pi}_S$ containing K column vectors of $\boldsymbol{\Pi}$ corresponding to the K dominant singulars. The next step is to obtain $\boldsymbol{\Pi}_{S,1}$ or $\boldsymbol{\Pi}_{S,2}$ by deleting the last row or the first row of $\boldsymbol{\Pi}_S$, respectively. The spectrum components z_k of the whole system can be derived by calculating the eigenvalues of the $K \times K$ matrix $\boldsymbol{\Pi}_{S,2}^H\left[\boldsymbol{\Pi}_{S,1}^H\right]^\dagger$.

Note that the spectrum components of the whole system may be different from the spectrum components obtained from the observation vector of each individual PMU. Inter-area oscillations can be detected by analyzing the aggregated matrix $\boldsymbol{B}$ of the entire system, while local oscillations may be detected only in some observation matrices.

Bear in mind that K is usually a small number and the computational complexity of calculating the eigenvalues of a $K \times K$ matrix is low. Nonetheless, the computational complexity of the matrix pencil method mainly depends on the implementation of SVD, which is on the order of $O((N-L)^3)$ or $O((\mathrm{P}(N-L))^3)$. Such a high complexity makes the SVD rather impractical to be run in recursive mode. Alternatively, the fast data projection method (FDPM) algorithm proposed in Ref. 27 can be used to recursively update and track the signal subspace $\boldsymbol{V}_S$ or $\boldsymbol{\Pi}_S$ on a sample-by-sample fashion. Bear in mind that $\boldsymbol{V}$ in Eq. (6) is an orthonormal matrix that consists of eigenvectors of $\boldsymbol{Y}^H\boldsymbol{Y}$, which can be decomposed into a signal subspace $\boldsymbol{V}_S$ and a noise subspace $\boldsymbol{V}_n$ as $\boldsymbol{Y}^H\boldsymbol{Y} = \boldsymbol{V}\boldsymbol{\Lambda}\boldsymbol{V}^H = \begin{bmatrix} \boldsymbol{V}_s & \boldsymbol{V}_n \end{bmatrix} \begin{bmatrix} \boldsymbol{\Lambda}_s & 0 \\ 0 & \boldsymbol{\Lambda}_n \end{bmatrix} \begin{bmatrix} \boldsymbol{V}_s^H \\ \boldsymbol{V}_n^H \end{bmatrix}$, where $\boldsymbol{V}_S$ is also the signal subspace in Eq. (7), which can be updated and tracked by the FDPM algorithm. Similar processing can be implemented on $\boldsymbol{\Pi}_S$.

III. FAST SUBSPACE TRACKING ALGORITHM

The FDPM is a numerically stable algorithm for subspace tracking with the ability to quickly converge to the steady-state.[32] In our proposed subspace tracking algorithm, the m th $(N-L)\times(L+1)$ observation output matrix $\boldsymbol{Y}(m)$ is constructed as

$$\boldsymbol{Y}(m) = \begin{bmatrix} y(0+m) & y(1+m) & \cdots & y(L+m) \\ y(1+m) & y(2+m) & \cdots & y(L+1+m) \\ \vdots & \vdots & \ddots & \vdots \\ y(N-L-1+m) & y(N-L+m) & \cdots & y(N-1+m) \end{bmatrix}. \tag{12}$$

We then implement an SVD to the output matrix $Y(0)$ and derive the initial subspace $V_S(0)$. The signal subspace $\boldsymbol{V}_S$ is updated and tracked using the FDPM algorithm shown in Table I.

In terms of the operational procedure of the FDPM algorithm, $\boldsymbol{V}_S(m)$ and $\mu(m)$ represent the signal subspace and a normalized step size at the m th time instant, respectively, which are used to guarantee the convergence of the FDPM algorithm. The exponential forgetting factor $0 < \nu \le 1$ is applied to down-weigh the previous data. This is used to track the statistical variation of the observed data when working in a nonstationary environment. By projecting the $(L+1)\times(N-L)$ dimensional observation matrix $\boldsymbol{Y}^H$ to the noise subspace, the modified FDPM algorithm is capable of recursively updating and tracking the subspace of the covariance matrix $\boldsymbol{Y}^H\boldsymbol{Y}$ on a sample-by-sample basis. A $K\times(N-L)$ dimensional matrix $\boldsymbol{E}_1 = \boldsymbol{e}_1 \times [1\,1 \cdots 1]$, $\boldsymbol{e}_1 = [1\,0 \cdots 0]^H$ is used to update the signal subspace. Householder transformation $\boldsymbol{I} - \frac{2\boldsymbol{A}_n(m)\boldsymbol{A}_n^H(m)}{\|\boldsymbol{A}_n m\|^2}$ is then used to orthonormalize the signal subspaces $\boldsymbol{V}_S(m)$, which can play a crucial role in the stability and the robustness of the process.

Based on the updated signal subspace $\boldsymbol{V}_S(m)$, we can obtain the signal subspace $\boldsymbol{V}_{S,1}^H(m)$ and $\boldsymbol{V}_{S,2}^H(m)$. After deriving the spectrum components $z_1, z_2, \cdots, z_K$ by calculating the eigenvalues of the $\boldsymbol{V}_{S,2}^H(m)\left[\boldsymbol{V}_{S,1}^H(m)\right]^\dagger$, amplitude A_i can be derived by solving Eq. (4).

When considering spectrum tracking for the entire power grid system, the aggregated $P(N-L)\times(L+1)$ output matrix $\boldsymbol{B}$ is used. The FDPM algorithm is modified to recursively update and track the subspace of the covariance matrix $\boldsymbol{B}^H\boldsymbol{B}$ on a sample-by-sample fashion. As shown in Table I, $\boldsymbol{B}^H(m)$ is the m th aggregated matrix and $\boldsymbol{\Pi}_S(m)$ represents the signal subspaces at the m th time instant. Instead of projecting the output matrix $\boldsymbol{Y}^H(m)$ to the signal subspace $\boldsymbol{V}_S(m-1)$, we project the $(L+1)\times P(N-L)$ matrix, $\boldsymbol{B}^H(m)$, to update the signal subspace $\boldsymbol{\Pi}_S(m-1)$.

The FDPM algorithm is able to converge to an orthonormal matrix despite being initialized with a non-orthonormal one.[27] Furthermore, it exhibits the fastest convergence rate among subspace

TABLE I. Procedure of the FDPM algorithm for tracking subspaces of the observation matrix $\boldsymbol{Y}$ or $\boldsymbol{B}$.

Updating the signal subspace $\boldsymbol{V}_s$ or $\boldsymbol{\Pi}_S$ and tracking oscillation components z_k.
Perform an SVD to the initial output matrix $\boldsymbol{Y}(0)$ or $\boldsymbol{B}(0)$ and generate the initial signal subspace $\boldsymbol{V}_S(0)$ or $\boldsymbol{\Pi}_S(0)$.
Calculate $\mu(0) = \frac{\overline{\mu}}{\|\boldsymbol{Y}(0)\|^2}$ or $\mu(0) = \frac{\overline{\mu}}{\|\boldsymbol{B}(0)\|^2}$, where $\overline{\mu}$ is a constant parameter less than 1.
For $m = 1, 2, \ldots$ Do
1. Update $\mu(m) = \frac{\overline{\mu}\cdot\mu(m-1)}{\nu\overline{\mu}+(1-\nu)\|\boldsymbol{Y}(m)\|^2\mu(m-1)}$ or $\mu(m) = \frac{\overline{\mu}\cdot\mu(m-1)}{\nu\overline{\mu}+(1-\nu)\|\boldsymbol{B}(m)\|^2\mu(m-1)}$, where ν is the forgetting factor,
2 . $\boldsymbol{R}_n(m) = \boldsymbol{V}_S{}^H(m-1)\boldsymbol{Y}^H(m)$ or $\boldsymbol{R}_n(m) = \boldsymbol{\Pi}_S{}^H(m-1)\boldsymbol{B}^H(m)$: projecting the matrix $\boldsymbol{Y}^H(m)$ or $\boldsymbol{B}^H(m)$ to the signal subspace,
3 . $\boldsymbol{T}_n(m) = \boldsymbol{V}_S(m-1) + \mu(m)\boldsymbol{Y}^H(m)\boldsymbol{R}_n^H(m)$ or $\boldsymbol{T}_n(m) = \boldsymbol{\Pi}_S(m-1) + \mu(m)\boldsymbol{B}^H(m)\boldsymbol{R}_n^H(m)$,
4 . $\boldsymbol{A}_n(m) = \boldsymbol{R}_n(m) - \|\boldsymbol{R}_n(m)\|\boldsymbol{E}_1$,
5. $\boldsymbol{Z}_n(m) = \boldsymbol{T}_n(m) - \frac{2}{\|\boldsymbol{A}_n(m)\|^2}\boldsymbol{T}_n(m)\boldsymbol{A}_n(m)\boldsymbol{A}_n^H(m)$,
6. $\boldsymbol{V}_S(m) = normalize\{\boldsymbol{Z}_n(m)\}$ or $\boldsymbol{\Pi}_S(m) = normalize\{\boldsymbol{Z}_n(m)\}$: updating the signal subspace.
7. Obtain $\boldsymbol{V}_{S,1}(m)$ or $\boldsymbol{V}_{S,2}(m)$ $[\boldsymbol{\Pi}_{S,1}(m)$ or $\boldsymbol{\Pi}_{S,2}(m)]$ by deleting the last row or the first row of $\boldsymbol{V}_S(m)$ $[\boldsymbol{\Pi}_S(m)]$, respectively.
8. Derive the spectrum components $z_1, z_2, \cdots, z_K$ by calculating the eigenvalues of the $K\times K$ matrix $\boldsymbol{V}_{S,2}^H(m)\left[\boldsymbol{V}_{S,1}^H(m)\right]^\dagger$ or $\boldsymbol{\Pi}_{S,2}^H(m)[\boldsymbol{\Pi}_{S,1}^H(m)]^\dagger$.
9. Calculate the amplitude A_i by solving Eq. (4).

tracking algorithms with computation complexity on the order of $O((L+1)K)$.

IV. FAST AND LOW-COMPLEXITY TRACKING ALGORITHM

In Ref. 33, a low-complexity fast tracking algorithm is proposed to track the harmonics, sub-harmonics and inter-harmonics in power grid systems. This algorithm has a very low complexity of $O(K)$, where K is the model order of observation vectors. Because of its low complexity and fast tracking characteristics, it is re-designed to track low frequency oscillations.

Based on Eq. (3), the ambient PMU measurements can be expressed as

$$y(t) = \sum_{i=1}^{K} A_i e^{\alpha_i t} \sin(2\pi f_i t + \varphi_i) + n(t). \tag{13}$$

Gradient descent methods are used to minimize the least squares error between measurement $y(t)$ and the desired signal $A_i e^{\alpha_i t} \sin(2\pi f_i t + \varphi_i)$.[34] The objective is to extract the desired signal from $y(n)$. The manifold containing all sinusoidal signals in $y(t)$ can be expressed as $\mathcal{M}$;

$$\mathcal{M} = \{A(t) e^{\alpha(t)t} \sin(2\pi f(t)t + \varphi(t))\}, \tag{14}$$

where $A(t) \in [A_{\min}, A_{\max}]$, $\alpha(t) \in [\alpha_{\min}, \alpha_{\max}]$, $f(t) \in [f_{\min}, f_{\max}]$, and $\varphi(t) \in [\varphi_{\min}, \varphi_{\max}]$. Please note that damping factor, α, is an important parameter used to assess low frequency oscillations. It should be estimated and tracked in time. The parameter vector belonging to parameter space, $\Phi = [A, \alpha, f, \varphi]$, can be expressed as;

$$\phi(t) = [A(t), \alpha(t), f(t), \varphi(t)]^T, \tag{15}$$

where T denotes matrix transposition. We define a desired sinusoidal component as follows:

$$y(t, \phi(t)) = A(t) e^{\alpha(t)t} \sin(2\pi f(t)t + \varphi(t)). \tag{16}$$

To extract any desired component, such as the ith order of signals from $y(t)$, we need to identify an optimum ϕ_i, $i = 1, 2, \ldots, K$, according to the following equation;

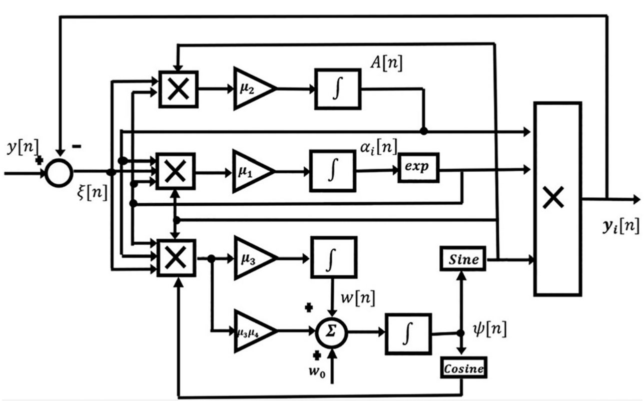

FIG. 3. Block diagram of the low complexity tracking algorithm.

$$\phi_i = \arg \min_{\phi_i(t) \in \Phi} d\left[y(t, \phi_i(t)), \left(y(t) - \sum_{j=1, j\neq i}^{K} z_j \right) \right], \tag{17}$$

where $d[y(t, \phi_i(t)), \left(y(t) - \sum_{j=1, j\neq i}^{K} z_j\right)]$ is the distance function between $y(t, \phi_i(t))$ and $y(t) - \sum_{j=1, j\neq i}^{K} z_j$, while $z_j = A_j e^{\alpha_j t} \sin(2\pi f_j t + \varphi_j)$ is the estimated component of the jth order of signals. Based on (17), the corresponding cost function can be shown as;

$$\mathcal{J}(t, \phi(t)) = d^2(t, \phi(t)) \triangleq e^2(t) = \left[y(t) - \sum_{j=1, j\neq i}^{K} z_j \right]^2. \tag{18}$$

The gradient decent method is then used to estimate parameter vector ϕ;

$$\frac{d\phi(t)}{dt} = -\Upsilon \frac{\partial[\mathcal{J}(t, \phi(t))]}{\partial \phi(t)}, \tag{19}$$

where the positive diagonal matrix, Υ, is the algorithm regulating constant matrix. Denote the estimated value of parameter vector as;

$$\hat{\phi}(t) = [\hat{A}(t), \hat{\alpha}(t), \hat{f}(t), \hat{\varphi}(t)]^T,$$

where $\hat{A}(t)$, $\hat{\alpha}(t)$, $\hat{f}(t)$, and $\hat{\varphi}(t)$ are estimated values of amplitude, damping factor, frequency, and phase, respectively.

Based on Eq. (19), we can derive the estimation for damping factor α as;

$$\begin{aligned} \frac{d\hat{\alpha}(t)}{dt} &= \mu_1 \frac{\partial}{\partial \hat{\alpha}(t)} \left[y(t) - \hat{A}(t) e^{\hat{\alpha}(t)t} \sin\left(2\pi \hat{f}(t)t + \hat{\varphi}(t)\right) \right]^2 \\ &= 2\mu_1 \xi(t) \hat{A}(t) e^{\hat{\alpha}(t)t} \sin\left(2\pi \hat{f}(t)t + \hat{\varphi}(t)\right), \end{aligned} \tag{20}$$

where $\xi(t) = y(t) - \hat{A}(t) e^{\hat{\alpha}(t)t} \sin\left(2\pi \hat{f}(t)t + \hat{\varphi}(t)\right)$ and μ_1 is a constant step value. The nonlinear differential equation for damping factor, α_i, of the ith spectrum component can be written as;

$$\dot{\hat{\alpha}}_i = 2\mu_1^i \xi \hat{A}_i e^{\hat{\alpha}_i t} \sin\hat{\psi}_i, \tag{21}$$

where $\hat{A}_i$ is the estimation of amplitude A_i, $\hat{\alpha}_i$ is the estimation of the damping factor α_i, $\hat{\omega}_i$ is the estimation of frequency $\omega_i = 2\pi f_i$, $\hat{\psi}_i$ is the estimation of total phase $\psi_i = \omega_i t + \varphi_i$, and $\xi = y(n) - \sum_{i=1}^{M} \hat{A}_i e^{\hat{\alpha}_i t} \sin\hat{\psi}_i$ is the error signal between the PMU measurement, $y(n)$, and its estimation. Similarly, a set of nonlinear differential equations for other parameters can be derived as;

$$\dot{\hat{A}}_i = 2\mu_2^i \xi e^{\hat{\alpha}_i t} \sin\hat{\psi}_i, \tag{22}$$

$$\dot{\hat{\omega}}_i = 2\mu_3^i \xi \hat{A}_i e^{\hat{\alpha}_i t} \cos\hat{\psi}_i, \tag{23}$$

$$\dot{\hat{\psi}}_i = \hat{\omega}_i + 2\mu_3^i \mu_4^i \xi \hat{A}_i e^{\hat{\alpha}_i t} \cos\hat{\psi}_i. \tag{24}$$

Step parameters μ_1^i and μ_2^i are used to control the convergence speed and accuracy of the ith component's amplitude and damping factor, respectively.[35] Step parameters μ_3^i and μ_4^i are pre-set to get a trade-off between convergence speed and accuracy of the ith frequency

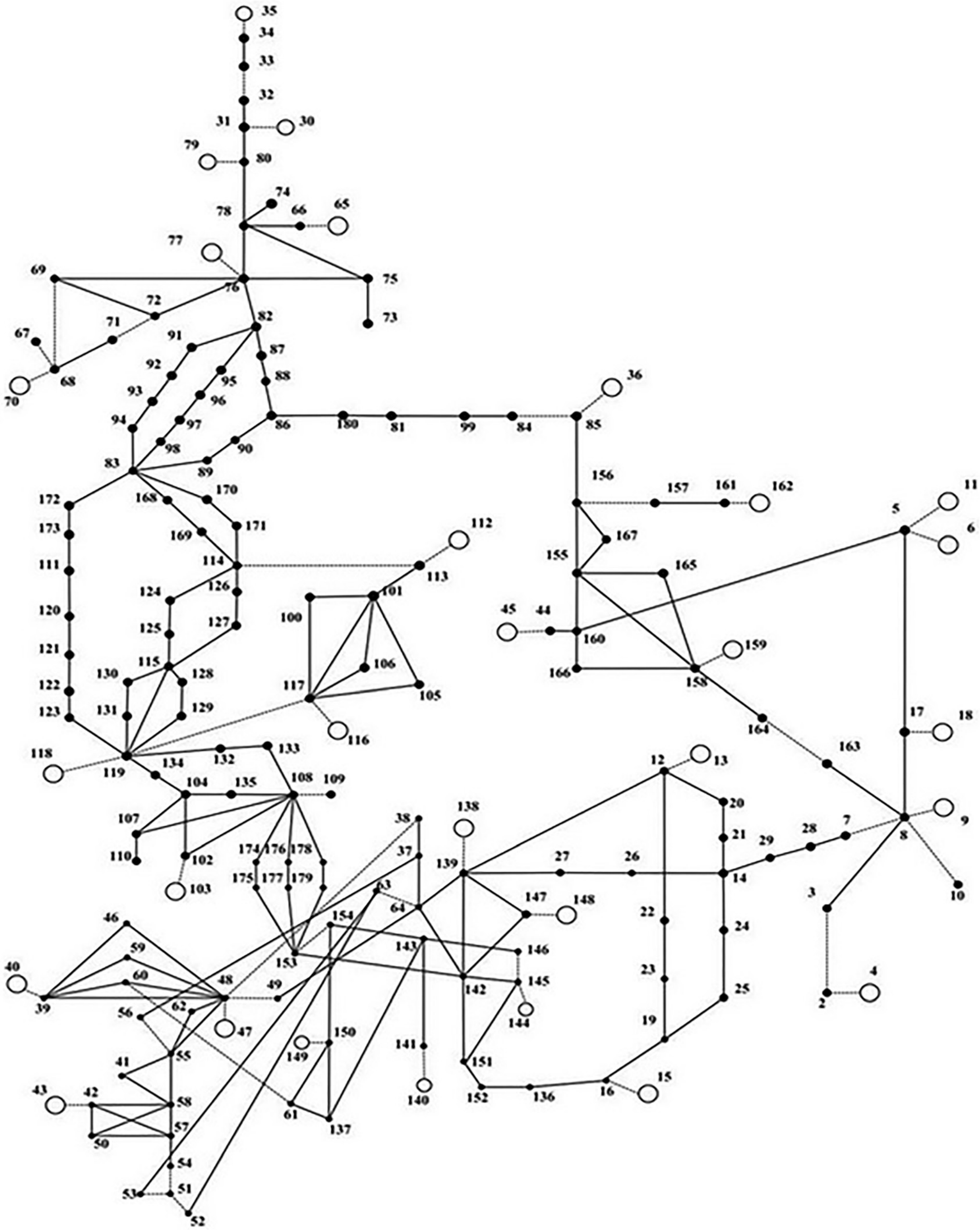

FIG. 4. A simplified WECC 179-bus power system.

component. Based on first order time derivative approximation, the discretized form of Eqs. (21)–(24) can be written as

$$\alpha_i[n+1] = \alpha_i[n] + 2T_s\mu_1^i\xi[n]A_i[n]e^{\alpha_i[n]nT_s}\sin(\psi_i[n]), \tag{25}$$

$$A_i[n+1] = A_i[n] + 2T_s\mu_2^i\xi[n]e^{\alpha_i[n]nT_s}\sin(\psi_i[n]), \tag{26}$$

$$\omega_i[n+1] = \omega_i[n] + 2T_s\mu_3^i\xi[n]A_i[n]e^{\alpha_i[n]nT_s}\cos(\psi_i[n]), \tag{27}$$

$$\psi_i[n+1] = \psi_i[n] + T_s\omega_i[n] + 2T_s\mu_3^i\mu_4^i\xi[n]A_i[n]e^{\alpha_i[n]nT_s}\cos(\psi_i[n]), \tag{28}$$

$$y_i[n] = A_i[n]e^{\alpha_i[n]nT_s}\sin(\psi_i[n]), \tag{29}$$

while the error signal can be expressed as

$$\xi[n] = y[n] - \sum_{i=1}^{K} A_i[n] e^{\alpha_i[n] n T_s} \sin(\psi_i[n]), \tag{30}$$

where n is the time step index and T_s is the sampling interval. The implementation of the proposed tracking algorithm is displayed in Fig. 3.

By appropriately setting the initial values of the spectrum components, the proposed algorithm is capable of simultaneously tracking multiple components. In order to achieve a reliable performance while maintaining low complexity, the proposed algorithm is based on a combination of the matrix pencil method (see Sec. II) and the low complexity tracking algorithm, as described in this section. Specifically, in the initial stage, the matrix pencil method is first performed to acquire prior knowledge of all spectrum components and their corresponding initial values. This information is then used by the low complexity tracking algorithm to track and monitor the oscillation components in recursive mode. Furthermore, with the help of the matrix pencil method on the spectrum of the whole system, the proposed tracking algorithm can easily identify and track the inter-area oscillations. Otherwise, detecting inter-area oscillations would require crosschecking low frequency oscillation from all the PMUs.

In the case of changing oscillations, their frequency estimations will undergo significant fluctuations. Here, the matrix pencil method will be invoked to re-calculate the oscillation components. In this way, the computational complexity of the proposed algorithm is mainly based on the low complexity tracking algorithm, which is on the order of $O(K)$.

After identifying the oscillation frequencies by using the matrix pencil method, the components of the observation PMU vector, $\boldsymbol{y}$, can be filtered by K Gaussian filters at $f_1, f_2, \ldots, f_K$ with deviation σ_i, to generate approximation of K oscillation components:

$$\boldsymbol{y}_i = \boldsymbol{y} * \boldsymbol{g}_i, \quad i = 1, 2, \ldots, K, \tag{31}$$

where "$*$" is the linear convolution operation. The Gaussian bandpass filter $\boldsymbol{g}_i$'s frequency response is given by

$$\boldsymbol{g}_i(f) = \frac{e^{-\frac{(f-f_i)^2}{2(\sigma_i)^2}}}{\sqrt{2\pi}\sigma_i}. \tag{32}$$

The proposed low complexity tracking algorithm is then applied to the filtered signal, $\boldsymbol{y}_i$, to enhance performance, hence mitigating any interference from other oscillation components.

V. SIMULATION RESULTS

In this section, we assess the performance of the proposed fast tracking algorithms by using: a test signal, a simplified WECC 179-bus power system from a test case library[36] shown in Fig. 4, and some actual PMU data sets with oscillatory events captured in ISO New England power systems.

In Figs. 5–7, the following test signal is used: $y(t) = e^{-0.05t} \sin(2\pi \times 0.2t) + e^{-0.1t}\sin(2\pi \times 0.3t) + n(t)$, where $n(t)$ is the AWGN and $y(t)$ is sampled at 30 Hz. The test signal contains two oscillation modes at 0.2 and 0.3 Hz with a damping ratio of 3.98% and 5.30%, respectively. Signal to noise ratios (SNRs) of 20 and 30 dB, have been used in our experiments. In the case of the fast subspace tracking algorithm, we have $N = 600$ and $L = 300$. Figure 5 shows that both

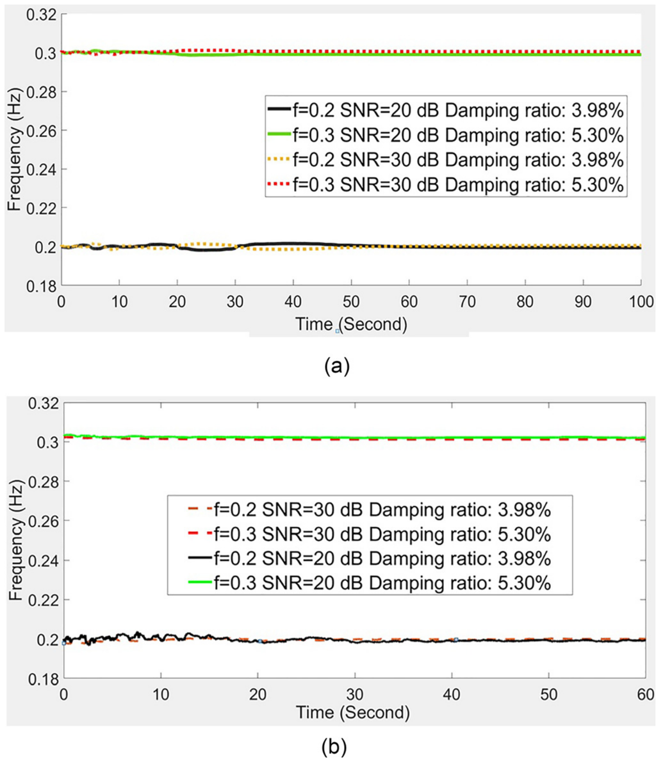

FIG. 5. The low frequency tracking performance of the proposed tracking algorithms on a test signal: (a) the gradient descent based low complexity tracking algorithm, (b) the fast subspace tracking algorithm.

algorithms are capable of accurately detecting and monitoring low frequency oscillations in the presence of noise. Figure 6 displays the damping factor tracking performance of the gradient descent based low complexity tracking algorithm on the test signal where initial damping factors α of 0.04 and 0.11 have been used for both oscillatory modes at 0.2 and 0.3 Hz, respectively [also see Eqs. (18)–(23)].

Figure 7 shows the performance of both tracking algorithms under changing oscillation frequencies. Specifically, the oscillation

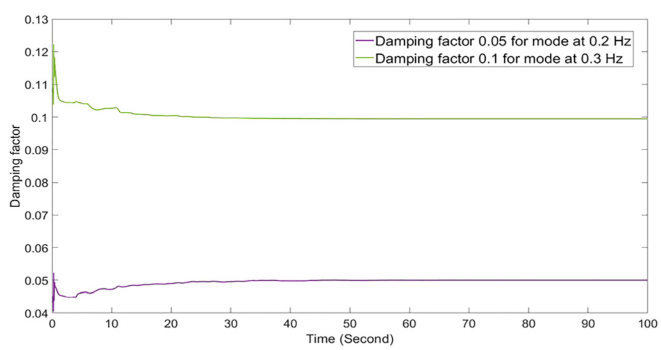

FIG. 6. The damping factor tracking performance of the gradient descent based low complexity tracking algorithm on a test signal where the initial damping factor α are 0.04 and 0.11 for modes at 0.2 and 0.3 Hz, respectively.

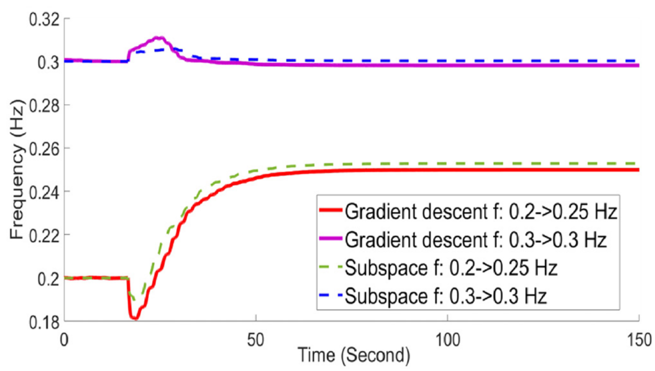

FIG. 7. The oscillation tracking performance of the low complexity tracking algorithms on a test signal where the oscillation mode at 0.2 Hz jumps to 0.25 Hz at time 16.67 s, while the other mode remains at 0.3 Hz.

mode at 0.2 Hz jumps to 0.25 Hz after 16.67 s, while the other mode remains at 0.3 Hz. These results demonstrate that both algorithms can track oscillations under changing oscillation frequencies.

In our next experiment, a simplified WECC 179-bus power system[36] (see Fig. 4) is used to generate PMU measurement data, where the sampling rate is 30 Hz. A three-phase short circuit fault is produced at 0.5 s on bus 159 and then cleared after 0.05 s. This results in a low frequency oscillation at 1.41 Hz with a low damping ratio of 1.0%. PMU data (sampled at 30 Hz), are collected for our experiment. In Fig. 8, two different sample-by-sample sliding windows sizes have been used to evaluate the accuracy of the fast subspace tracking algorithm. As shown in Fig. 8, a larger window size results in a better performance. This is mainly due to the fact that a larger window size can reduce the variance of frequency estimations, hence further improving the accuracy. Figure 8 also indicates that the gradient descent-based tracking algorithm, despite its lower complexity, is able to fast track the low frequency oscillation with a greater accuracy.

In our next experiment we have used actual PMU data sets capturing oscillatory events in ISO New England power systems, which is impacted by an inter-area natural oscillation at 0.27 Hz (due to the presence of a large generator). The collected PMU measurements

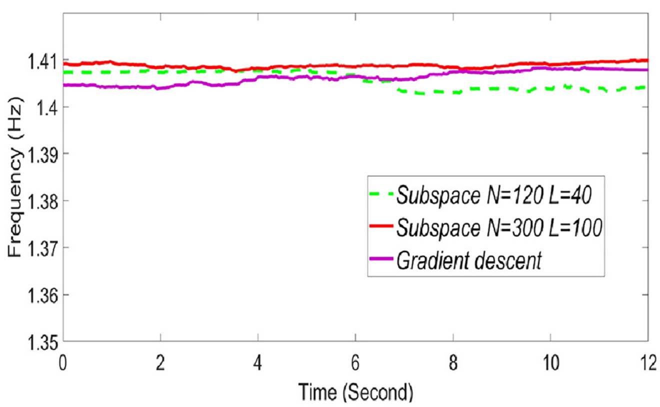

FIG. 8. The low frequency tracking performance of the proposed subspace tracking algorithm on a 1.41 Hz natural oscillation.

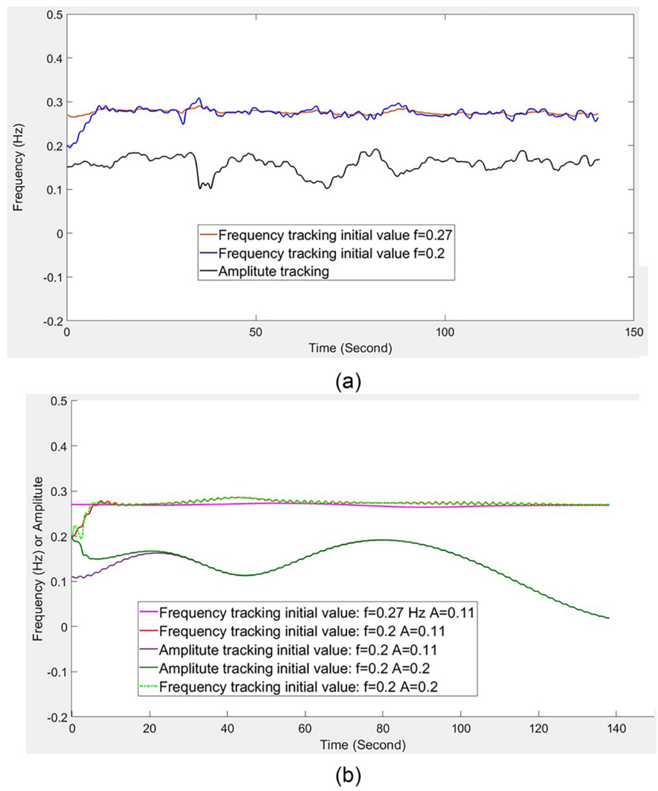

FIG. 9. The low frequency tracking performance of the gradient descent based low complexity tracking algorithm on actual PMU data sets capturing oscillatory events in ISO New England power systems, where the oscillation frequency is 0.27: (a) The PMU measurements are not filtered; (b) The PMU measurements are prefiltered by using Gaussian filter and different initial value is used to evaluate the tracking performance.

shown in Fig. 2 are sampled at 30 Hz.[36] Figure 9 displays the performance of the gradient descent based low complexity tracking algorithm when using the filtered or unfiltered PMU measurements. As can be observed, the gradient descent algorithm can significantly

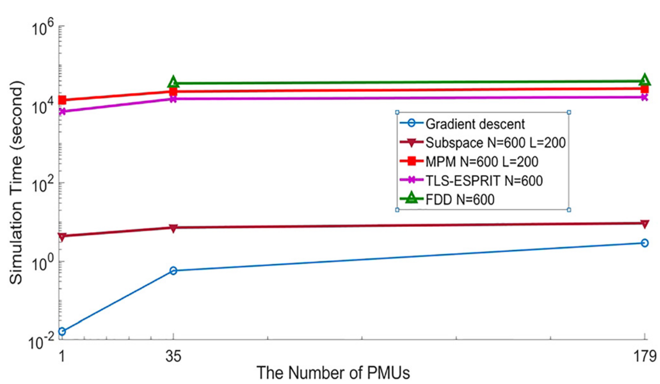

FIG. 10. Computation time of difference methods monitoring low frequency oscillations in a sample-by-sample fashion.

TABLE II. Comparison of the low complexity tracking algorithms with FDD[20] and TLS-ESPRIT.[24]

Method	FDD	TLS-ESPRIT	MPM	Subspace	Gradient descent
Freq. mean (Hz)	0.200 3	0.200 2	0.200 2	0.200 3	0.200 4
Freq. STD (Hz)	0.002 4	0.002 3	0.002 1	0.002 3	0.003 1
Damp. ratio mean (%)	3.87	3.88	3.95	3.93	3.92
Damp. ratio STD (%)	1.14	1.12	1.10	1.12	1.17
Freq. mean (Hz)	0.301 2	0.300 9	0.300 7	0.301 0	0.301 5
Freq. STD (Hz)	0.005 3	0.005 6	0.004 9	0.005 7	0.006 6
Damp. ratio mean (%)	5.82	5.49	5.38	5.42	5.58
Damp. ratio STD (%)	1.82	1.21	1.15	1.20	1.25

TABLE III. Comparison of the complexity of the proposed algorithms with some of the state of the art algorithms.

	Prony analysis, Kalman filter, FDD YWS N4SID ESPRIT MPM	RRLS R3LS	HHT AR ARMA	WT LMS	The subspace method	The gradient descent method
Complexity	$O(N^3)$	$O(N^2)$	$O(N\log N)$	$O(N)$	$O((L+1)K)$	$O(K)$

improve the tracking performance with the help of Gaussian filter. Furthermore, different initial values are used to demonstrate the convergence capability of the proposed algorithm. Note that there are some error data in the actual PMU data caused by communication error or delay. In the proposed algorithms, the lost PMU data can be easily detected by checking PMU's ID and the corresponding timestamp. If there is no measurement at a specific time, zero will be used. Figure 9 demonstrates the robustness of the proposed methods.

Figure 10 displays the computation time of different methods when monitoring a 500 s long PMU data from different PMU sets, namely, a single PMU data, a 35 PMUs data and a 179 PMUs data. It is shown that the gradient descent method achieves a significant speed advantage over the subspace method, the MPM Method, the FDD method[20] and the TLS-ESPRIT method[24] because of its extreme low computation complexity. The fast subspace method achieves the second best performance in computation time, due to the employed low complexity FPDM algorithm. Note that in Table II, the mean and standard deviation (STD) of frequency are expressed in Hz, while the STD of damping ratio are expressed in percentage (%). With the help of Gaussian filterer gradient descent method achieves a similar performance as the FDD method[20] and the TLS-ESPRIT method,[24] but with much lower computation complexity. The subspace method outperforms the gradient descent method at the expense of slightly increased complexity. It achieves a similar performance as the MPM method with significantly reduced complexity. In Table III, the complexity of the proposed algorithms is compared with the state of the art algorithms discussed in Sec. I.

VI. CONCLUSION

In this paper we investigate low frequency oscillation estimation and tracking for real-time power grid monitoring. We have demonstrated that the proposed fast subspace and the gradient descent based low complexity tracking algorithm can provide fast and reliable performance while maintaining low complexity. With the help of a Gaussian filter the gradient descent method is able to achieve a similar performance as the FDD method and the TLS-ESPRIT method, with much lower computation complexity. The subspace method outperforms the gradient descent method at the expense of slightly increased complexity. It achieves a similar performance as the MPM method with significantly reduced complexity. Furthermore, by using eigenvalue decomposition of the fast subspace tracking algorithm, the gradient descent based tracking algorithm can easily track inter-area oscillations. The simulation results demonstrate the robustness of the proposed low complexity tracking algorithms under dynamic conditions.

DATA AVAILABILITY

The data that support the findings of this study are available from the corresponding author upon reasonable request.

REFERENCES

[1] X. Zhang, C. Lu, S. Liu, and X. Wang, "A review on wide-area damping control to restrain inter-area low frequency oscillation for large-scale power systems with increasing renewable generation," Renewable Sustainable Energy Rev. **57**, 45–58 (2016).

[2] D. Cai, P. Regulski, M. Osborne, and V. Terzija, "Wide area inter-area oscillation monitoring using fast nonlinear estimation algorithm," IEEE Trans. Smart Grid **4**(3), 1721–1731 (2013).

[3] J. F. Hauer, D. J. Trudnowski, and J. G. DeSteese, "A perspective on WAMS analysis tools for tracking of oscillatory dynamics," in *Proceedings of IEEE Power Engineering Society General Meeting, 24–28 June* (IEEE, 2007), pp. 1–10.

[4] D. J. Trudnowski, J. W. Pierre, N. Zhou, J. F. Hauer, and M. Parashar, "Performance of three mode-meter block-processing algorithms for automated dynamic stability assessment," IEEE Trans. Power Syst. **23**(2), 680–690 (2008).

[5] G. Ledwich and E. Palmer, "Modal estimates from normal operation of power systems," in *Proceedings of IEEE Power Engineering Society Winter Meeting, 23–27 January* (IEEE, 2000), Vol. 2, pp. 1527–1531.

[6] R. W. Wies, J. W. Pierre, and D. J. Trudnowski, "Use of ARMA block processing for estimating stationary low-frequency electromechanical modes of power systems," IEEE Trans. Power Syst. **18**(1), 167–173 (2003).

[7] P. Korba, M. Larsson, and C. Rehtanz, "Detection of oscillations in power systems using Kalman filtering techniques," in *Proceedings of IEEE Conference on Control Applications CCA 2003, 23–25 June* (IEEE, 2003), Vol. 1, pp. 183–188.

[8] D. S. Laila, M. Larsson, B. C. Pal, and P. Korba, "Nonlinear damping computation and envelope detection using Hilbert transform and its application to power systems wide area monitoring," in *Proceedings of the IEEE PES General Meeting* (IEEE, 2009), pp. 1–7.

[9] J. L. Rueda, C. A. Juarez, and I. Erlich, "Wavelet-Based analysis of power system low-frequency electromechanical oscillations," IEEE Trans. Power Syst. **26**(3), 1733–1743 (2011).

[10] N. Zhou, J. W. Pierre, and J. F. Hauer, "Initial results in power system identification from injected probing signals using a subspace method," IEEE Trans. Power Syst. **21**(3), 1296–1302 (2006).

[11] G. Liu, J. Quintero, and V. Venkatasubramanian, "Oscillation monitoring system based on wide area synchrophasors in power systems," in IREP Symposium 2007, Charleston, SC (2007).

[12] S. A. Nezam Sarmadi and V. Venkatasubramanian, "Electromechanical mode estimation using recursive adaptive stochastic subspace identification," IEEE Trans. Power Syst. **29**(1), 349–358 (2014).

[13] H. Zhang, J. Ning, H. Yuan, and V. Venkatasubramanian, "Implementing Online oscillation monitoring and forced oscillation source locating at peak reliability," in *2019 North American Power Symposium (NAPS), Wichita, KS* (2019), pp. 1–6.

[14] J. W. Pierre, D. J. Trudnowski, and M. K. Donnelly, "Initial results in electromechanical mode identification from ambient data," IEEE Trans. Power Syst. **12**(3), 1245–1251 (1997).

[15] N. Zhou, J. W. Pierre, and R. W. Wies, "Estimation of low-frequency electromechanical modes of power systems from ambient measurements using a subspace method," in 35th NAPS, Rolla, MO (2003).

[16] R. W. Wies, J. W. Pierre, and D. J. Trudnowski, "Use of least mean squares (LMS) adaptive filtering technique for estimating low-frequency electromechanical modes in power systems," in *IEEE Power Engineering Society General Meeting* (IEEE, 2004), pp. 1863–1870.

[17] N. Zhou, J. W. Pierre, D. J. Trudnowski, and R. T. Guttromson, "Robust RLS methods for online estimation of power system electromechanical modes," IEEE Trans. Power Syst. **22**(3), 1240–1249 (2007).

[18] N. Zhou, D. J. Trudnowski, J. W. Pierre, and W. A. Mittelstadt, "Electromechanical mode online estimation using regularized robust RLS methods," IEEE Trans. Power Syst. **23**, 1670–1680 Nov. (2008).

[19] C. Y. Shih, Y. G. Tsuei, R. J. Allemang, and D. L. Brown, "Complex mode indication function and its applications to spatial domain parameter estimation," Mech. Syst. Signal Process. **2**, 367–377 (1988).

[20] R. Brincker, L. Zhang, and P. Andersen, "Modal identification from ambient responses using frequency domain decomposition," in Proceedings of the 18th International Modal Analysis Conference (IMAC), San Antonio, TX, February 7–10, 2000.

[21] J. Zuo, Y. Shen, D. Chen, H. Guo, Z. Hu, and K. Zhang, "Low frequency oscillation mode source identification with wide-area measurement system," in *IEEE 3rd Conference on Energy Internet and Energy System Integration (EI2), Changsha, China* (IEEE, 2019), pp. 1525–1539.

[22] G. Liu and V. Venkatasubramanian, "Oscillation monitoring from ambient PMU measurements by frequency domain decomposition," in *Proceedings of IEEE International Symposium on Circuits and Systems* (2008), pp. 2821–2824.

[23] P. Tripathy, S. C. Srivastava, and S. N. Singh, "A modified TLS-ESPRIT based method for low-frequency mode identification in power systems utilizing synchrophasor measurements," IEEE Trans. Power Syst. **26**(2), 719–727 (2010).

[24] J. Chen, T. Jin, M. A. Mohamed, and M. Wang, "An adaptive TLS ESPRIT algorithm based on an SG filter for analysis of low frequency oscillation in wide area measurement systems," IEEE Access **7**, 47644–47654 (2019).

[25] J. G. Philip and T. Jain, "Analysis of low frequency oscillations in power system using EMO ESPRIT," Int. J. Electr. Power Energy Syst. **95**, 499–506 (2018).

[26] Y. Hua and T. K. Sarkar, "Matrix pencil method for estimating parameters of exponentially damped/undamped sinusoids in noise," IEEE Trans. Acoust. **38**(5), 814–824 (1990).

[27] X. Doukopoulos and G. Moustakides, "Fast and stable subspace tracking," IEEE Trans. Signal Process. **56**(4), 1452–1465 (2008).

[28] X. Wang and H. V. Poor, "Blind multiuser detection: A subspace approach," IEEE Trans. Inf. Theory **44**, 677–690 (1998).

[29] B. Yang, "Projection approximation subspace tracking," in *IEEE Transactions on Signal Processing*, 7 January 1995 (IEEE, 1995) Vol. 43, pp. 95–107.

[30] B. Yang, "An extension of the PASTd algorithm to both rank and subspace tracking," IEEE Trans. Signal Process. **2**, 179–182 (1995).

[31] G. Rogers, *Power System Oscillations* (Kluwer, New York, 2000).

[32] J.-P. Delmas, *Subspace Tracking for Signal Processing. Adaptive Signal Processing: Next Generation Solutions* (Wiley-IEEE, 2010), pp. 211–270.

[33] B. Hu and H. Gharavi, "A fast recursive algorithm for spectrum tracking in power grid systems," IEEE Trans. Smart Grid **10**(3), 2882–2891 (2019).

[34] A. A. Giordano, *Least Square Estimation with Applications to Digital Signal Processing* (John Wiley and Sons, New York, 1985).

[35] A. K. Ziarani, "Extraction of nonstationary sinusoids," Ph.D. dissertation (University of Toronto, Toronto, Canada, 2002).

[36] S. Maslennikov, B. Wang, Q. Zhang, F. Ma, X. Luo, K. Sun, and E. Litvinov, "A test cases library for methods locating the sources of sustained oscillations," in IEEE PES General Meeting, Boston, MA, July 17–21, 2016.